Article:
Raza, G, Amjad, M, Kaur, I et al. (1 more author) (2016) Stability and Aggregation Kinetics of Titania Nanomaterials under Environmentally Realistic Conditions. Environmental science & technology, 50 (16). pp. 8462-8472. ISSN 0013-936X

https://doi.org/10.1021/acs.est.5b05746

Stability and Aggregation Kinetics of Titania Nanomaterials under Environmentally Realistic Conditions

Ghulam Raza[*†] Muhammad Amjad[†, §] Inder Kaur[✧] Dongsheng Wen[*†]

† School of Process, Environmental and Materials Engineering, University of Leeds, Leeds, LS2 9JU, UK

✧ School of Geography, Earth and Environmental Sciences, University of Birmingham, Birmingham, UK

§ Department of Mechanical Engineering, University of Engineering and Technology Lahore (City Campus), Pakistan

Abstract: Nanoparticle morphology is expected to play a significant role in the stability, aggregation behaviour and ultimate fate of engineered nanomaterials in natural aquatic environments. The aggregation kinetics of ellipsoidal and spherical titanium dioxide (TiO_2) nanoparticles (NP) under different surfactant loadings, pH values and ionic strengths are investigated in this study. The stability results reveal that alteration of surface charge is the stability determining factor. Among five different surfactants investigated, sodium citrate and Suwannee river fulvic acid (SRFA) were the most effective stabilizers. It was observed that both types of NP were more stable in monovalent salts (NaCl and $NaNO_3$) as compared with divalent salts ($Ca(NO_3)_2$ and $CaCl_2$). The aggregation of spherical TiO_2 NP demonstrated a strong dependency on the ionic strength regardless of the presence of mono or divalent salts; while the ellipsoids exhibited a lower dependency on the ionic strength but is more stable . This work acts as a benchmark study towards understanding the fate of stabilized NP in natural environments that are rich in $Ca(CO_3)_2$, $NaNO_3$, NaCl and $CaCl_2$ along with natural organic matters.

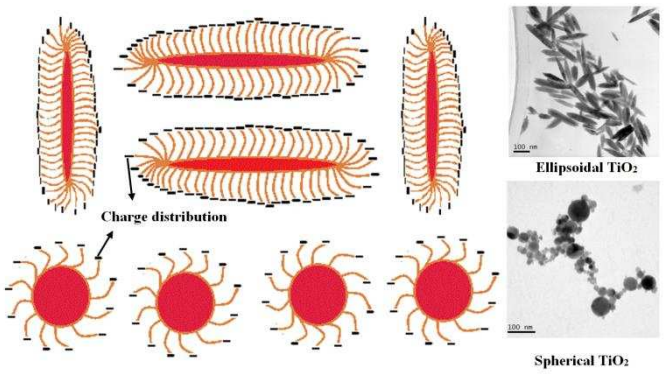

Keywords: Nanoparticle, stability, aggregation, kinetics, surfactants, sticking efficiency

INTRODUCTION

TiO_2 is a multipurpose material widely used in nano-particulate form[1]. TiO_2 nanoparticles (NP) are routinely used in products like sun creams, cosmetics, paints, self-cleaning dispersions, textiles, sports equipment, solar cells and waste water treatment devices[2]. Its unique properties give it an increased demand in different industries but at the same time causes increasing environmental concerns.

It is understood that the migration behaviour, toxicity and bioavailability of NP are governed by their physico-chemical properties such as shape, size, surface area, agglomeration state, zeta potential and surface chemistry[3, 4]. In the past decade, the aggregation kinetics of different NP has been extensively investigated[5-10]. As TiO_2 NP have the tendency to aggregate and coalesce into big particles, which is undesirable for most of the applications[11], their colloidal stability investigation becomes important[12, 13]. Most of the physico-chemical properties of NP are related to their behaviours in dispersions including the reactions at the particle–liquid interface[14].

To fully evaluate the environmental implications, the mobility and risks of such NPs, the knowledge regarding their interaction with different media constituents and the aggregation kinetics are essential. Several factors are responsible for NP aggregation as studied by different scientists[15-18]. Firstly, the surface charge of the NP greatly influence their solubility and hence the stability. Surface charge results in either attractive (positive-negative interaction) or repulsive (similar charge interactions) energies, which depend on the pH, temperature and the concentration and type of the electrolyte in the medium. The presence of electrolytes in the medium would alter the stability and agglomeration state of NP dispersions. Secondly, the concentration of the NP precursors, polymers, surfactants and the temperature would alter the overall stability of dispersions. Water or other molecules could interact with NP and alter their crystal structures. Zinc sulphide (ZnS) NP is a good example as reported by Zhang et al. (2003), where 3 nm ZnS NP containing around 700 atoms rearranged their crystal structures after the interaction with water to form more ordered bulk structure[19]. Guzman and co-workers[20] showed a pHzpc (i.e., pH at point of zero charge) dependence of titania NP while French et al.[21] observed the influence of ionic strength (IS), on the aggregation

kinetics of 50-60 nm TiO_2 agglomerates (with 5 nm primary size) at low IS. Similarly surface charge and zeta-potential has a strong correlation with the aggregation kinetics of ZnO NP[22]. In an interesting study on the aggregation kinetics[23], Suwannee river fulvic acid (SRFA)-stabilized TiO_2 NP showed strong stability at varying IS under acidic pH, while became aggregated under low IS at neutral pH values.

It shall be noted that many reported aggregation kinetic studies were based on colloids made from pre-fabricated nanomaterials[24-27], which inevitably contained many agglomerated NP due to the difficulty in dispersing them to their primary sizes. The aggregation kinetics, therefore, would be different to those well-dispersed colloids. The aggregation kinetics of NP is controlled by the electrostatic forces and the electrosteric interferences. The magnitude of the electrosteric interferences depends on the concentration of the stabilizing agent, coating thickness, the conformation and dimensions of the adsorbed double layer[17, 28]. From the environmental concern, the fate of NP in an aqueous system is dependent on both particle characteristics and the complex water chemistry such as pH, ionic strength and dissolved organic matter contents and properties, which may stabilize or agglomerate the NP influencing the transport of NP. Quite a few studies[29-32] have been conducted to investigate the effect of these influential factors, but no solid conclusion was reached and the understanding on the fate of NP under different environmental conditions is still very limited. Although there were a few studies on the transport of TiO_2 NP with particular reference to ionic strength and surfactants[33, 34], the influence of particle morphology is essentially lacking, hence the effects of ionic strength and surfactants on the aggregation kinetics are in-conclusive.

This work aims to address these limitations by conducting a detailed study of the stability and aggregation kinetics of stable TiO_2 NP and investigate the influence of particle morphology under environmental-like conditions. For this purpose, two different shaped TiO_2 colloids, i.e. ellipsoids and spherical NP, were synthesized. The aggregation kinetics of well-dispersed NP was assessed under five different stabilizing agents and four different ionic strengths. From the practical consideration,

78 the aggregation kinetics study was conducted at neutral pH values. This detailed study shall advance
79 the understanding in the ultimate fate of TiO_2 NP in complex environmental conditions.

80 MATERIALS AND METHODS

81 Materials preparation

82 All surfactants except Suwannee river fulvic acid (SRFA) were purchased from Sigma Aldrich and
83 used without further purification. SRFA was purchased from International Humic Substances Society
84 (Atlanta, USA) while HCl and NaOH (0.01-0.1M) were purchased from Fisher Scientific for pH
85 adjustment. Two types of titania NP were selected from many batches of self-fabricated lots. The only
86 precursor used in this research, i.e. 99% pure $TiCl_4$, was purchased from Sigma Aldrich. Briefly TiO_2
87 NP were synthesized by a modified hydrothermal methodology, similar to the one reported by Yin et
88 al[35]. In a typical synthesis, solution 1 was made by diluting $TiCl_4$ to 1mol/L with 5% HCl in an ice
89 bath. Solution 2 was prepared at different alcohol to water ratios (i.e., 1:2 Ethanol: Water, 1:2
90 Methanol: Water and 1:2 Acetone: Water). Both solutions 1 and 2 were mixed to get 0.1mol/L final
91 concentration of $TiCl_4$. Ice cooled temperature was maintained throughout the preparation process.
92 For rutile ellipsoids synthesis, the final dispersion was stirred for 30 minutes with magnetic stirrer at
93 45^{o}C temperature while for spherical anatase NP, the dispersion was treated at a temperature of 110^{o}C
94 for 40 minutes using Teflon lined vessels in a microwave oven (MARS 5). Finally three repetitive
95 washings with DI water and acetone were given to NP by centrifugation.

96 A 20 ml dispersion of 20 ppm spherical NP was stabilized with different surfactants including
97 polyethylene glycol (PEG), Polyvinylpyrrolidone (PVP), sodium dodecyl sulfate (SDS) and
98 Suwannee river fulvic acid (SRFA). The concentrations of all surfactants were optimized for spherical
99 NPs and similar concentrations were used for ellipsoids for all experiments. When stabilized in SRFA
100 and sodium citrate, rutile ellipsoids and anatase spherical NPs were tested for their aggregation
101 kinetics against different salt concentrations (NaCl, $NaNO_3$, $Ca(NO_3)_2$ and $CaCl_2$).

An advanced X-Ray diffraction spectroscopy (Bruker D-8, installed with PANalytical X'pert Pro software), Transmission electron microscope (TEM, Tecnai F-20) and Malvern Zetasizer (NanoZS90 5001) were used for NP characterization. For TEM study, rutile ellipsoids and anatase spherical NP were stabilized with 0.3% sodium citrate and SRFA100 (i.e., the concentration of SRFA is 100 ppm). Holey carbon film TEM copper grids were purchased from Agar Scientific. In a typical preparation process, the NP sample was diluted 100 times and a 10µl drop of the dilute was sandwiched between two DI water drops of 50µl. The grid was dried in a clean environment under room temperature and rinsed with DI water to remove any dirt or excessive materials. The grids for aggregation kinetics were prepared without diluting the samples, by following the same grid preparation methodology.

Time resolved aggregation kinetics

Time-resolved DLS (Dynamic Light Scattering) measurements of aggregating TiO_2 NP were performed at 20^0C except for the zeta potential, which were done at 25^oC as per Malvern instructions. The scattering angle was 90^o for all measurements. The concentration of the fabricated nanoparticles dispersion was measured by an atomic absorption spectrometer (AAS, Varian AA240FS) and a fixed TiO_2 concentration of 20 ppm was used via dilution in all experiments. In the experiments, 1 ml of nanoparticle dispersion was mixed with different amounts of mono or divalent dispersions in a mixing vial to reach desired concentration of electrolytes. The resulting dispersion was shaken gently and transferred quickly to DLS cuvettes for the measurement. Every reading was taken at 10 second interval with the maximum of 500 readings. The effect of pH, surfactants and zeta potential on the aggregation kinetics was studied for a period of 2 weeks.

The aggregation kinetics was derived from experimentally-measured particle size data. At the early stage, the formation of doublets (i.e., usually considered at the time where the initial aggregate hydrodynamic diameter increases by one quarter of its original size) was expressed in Eq.(1)[36]

$$\left(\frac{\Delta a_h(t)}{\Delta t}\right)_{t\to 0} \propto k_{11}N_0 \qquad (1)$$

where $a_h(t)$ is the aggregation size over time t, N_0 is the starting number concentration of NP dispersion and k_{11} is the rate of formation of doublets. These doublets increase in number at a faster rate with an increase in ion concentration in the dispersion due to the suppression of diffused double layer (DDL). This suppression of DDL leads to a decrease in the van der Waal forces between particles. At a point when all the van der Waal forces are overwhelmed, k_{11} becomes equal to the diffusion limited aggregation rate, i.e., k_{slow}, which shows the overall aggregation rate. The Smoluchowski aggregation rate, or k_{fast}, was calculated by Eq. (2)[37]

$$k_{fast} = 8kT/3u \quad (2)$$

where k represents Boltzmann's constant, u is the liquid's viscosity and T is the temperature. The sticking efficiency 'α' is defined as the ratio of k_{slow} and k_{fast}, as in Eq.(3), which is the average of the fastest points of aggregation stage at a specific ionic strength,

$$\alpha = \frac{k_{slow}}{k_{fast}} \quad (3)$$

and the critical coagulation concentration (CCC) is the concentration value when α approaches to a value of 1.

RESULTS AND DISCUSSION

TiO_2 characterization

The average length of rutile ellipsoids measured by TEM was 100±20nm (i.e. from randomly selected 214 ellipsoids) with average width of 20±5nm, which gives an aspect ratio of 4.5±0.3 and a hydrodynamic diameter of 55±5. The ellipsoids used for stability experiments were dispersed for a period over 6 months with no aggregation or agglomeration as measured by the DLS method. The spherical NP had a core size range between 60±35nm [38] and hydrodynamic diameter of 100±10nm for both citrate and SRFA100 stabilised. Figure 1a and 1b show TEM micrograph of SRFA stabilized rutile ellipsoids and spherical anatase NP respectively, with detailed morphology shown by HRTEM in Figure 1c and 1d. HRTEM micrograph of the rutile TiO2 (Figure 1c) shows lattice fringes with d-

spacing of 0.248nm, corresponding to (101) plane, and 0.324nm, corresponding to (110) of the rutile phase. HRTEM micrograph of the anatase TiO_2 (Figure 1d) shows lattice fringes with d-spacing of 0.189 nm, which corresponds to the (200) plane, 0.352nm corresponding to (101) plane and 0.290nm (121) planes of the anatase phase. Figures 2a and 2b illustrate the hydrodynamic particle size distribution of TiO_2 ellipsoids and spherical NP in water respectively.

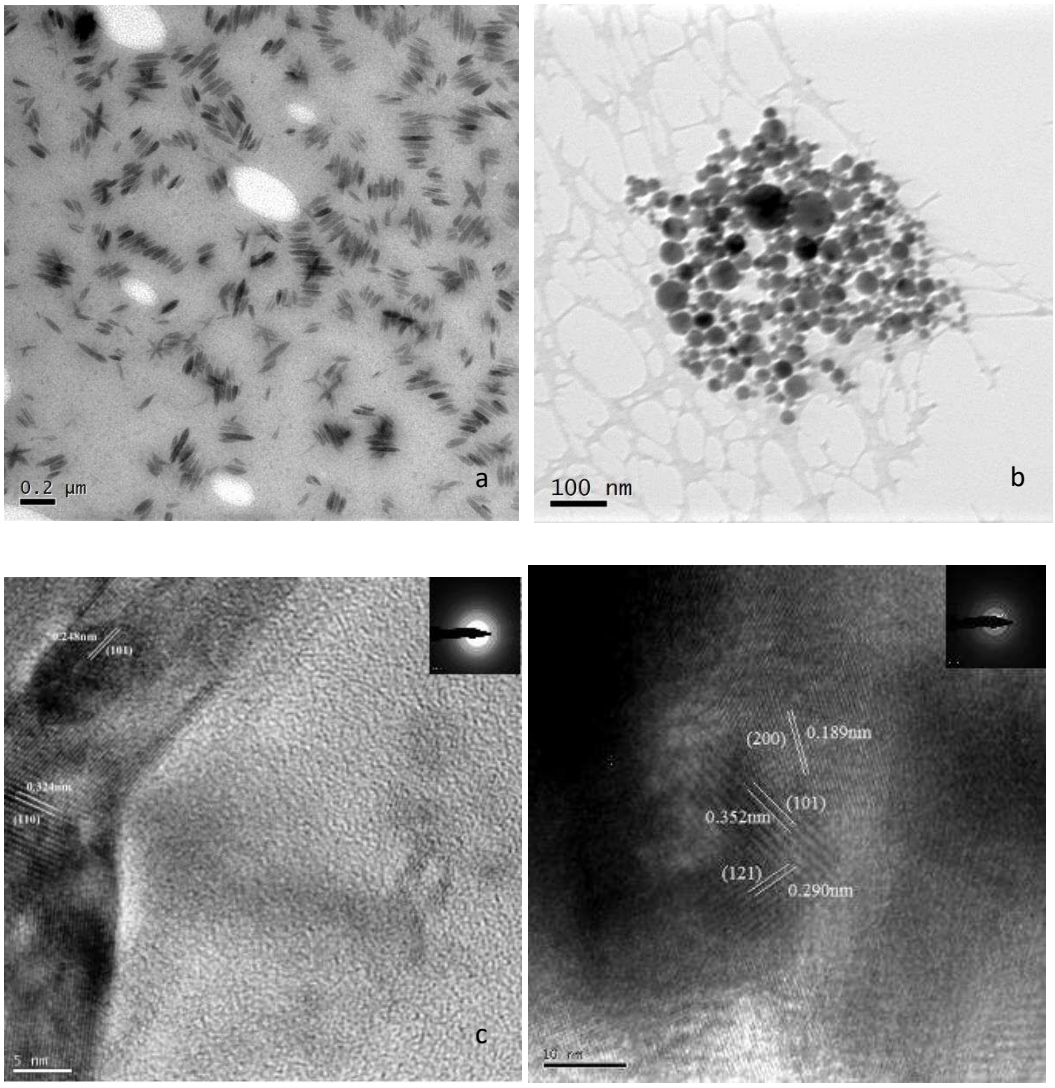

Figure 1: a) TEM micrograph of TiO_2 ellipsoids dispersed with SRFA100; b) Spherical anatase NP stabilized with SRFA100; c) HRTEM of TiO_2 ellipsoids with SAED pattern showing lattice fringes (101) and (110); d) HRTEM of spherical anatase with SAED pattern showing lattice fringes (101), (200) and (121)

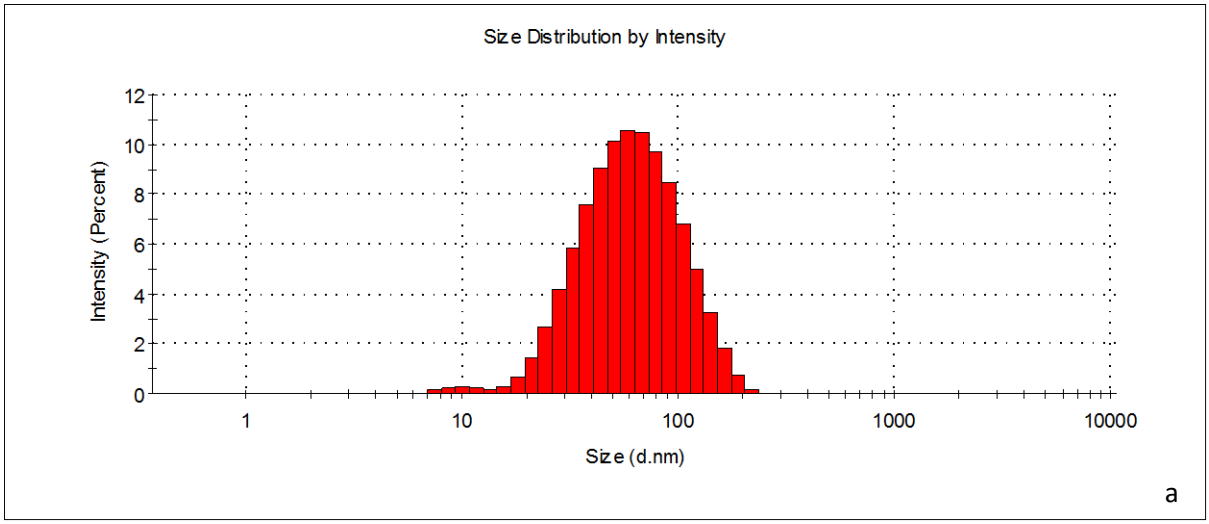

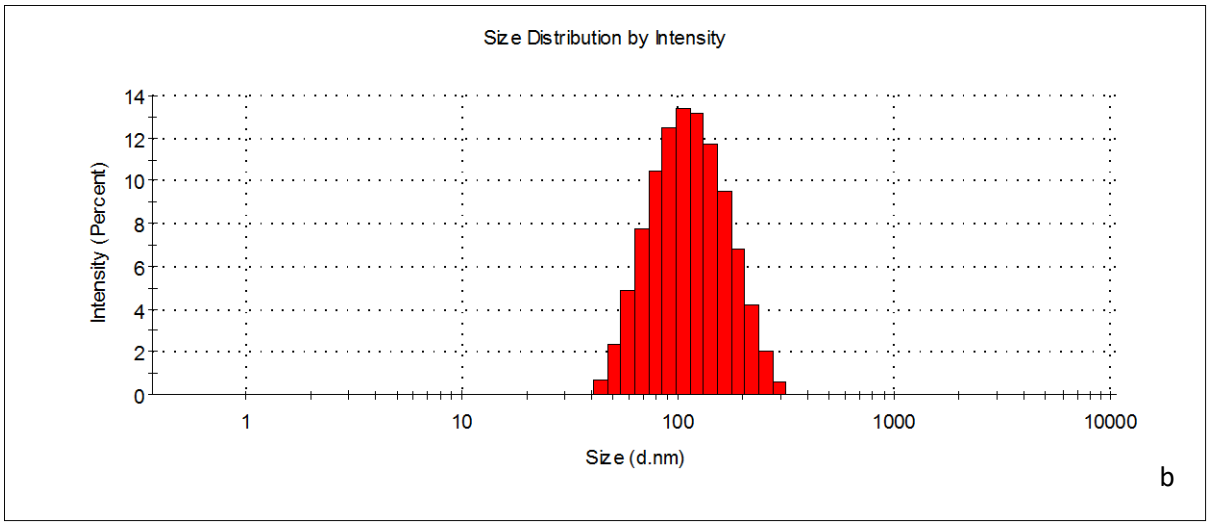

Figure 2: a) DLS histogram of TiO_2 ellipsoids dispersed with SRFA100 and b) DLS histogram of spherical anatase NP stabilized with SRFA100. (All measurements were taken at pH 6.5±0.2 without any electrolyte).

Impact of surface functionalization on the stability of TiO_2

Spherical anatase NPs were tested for their stability at different pH values in the presence of different surfactants. Results from different surfactants treatment revealed a change in size and zeta potential over a period of 2 weeks. The dispersion without surfactants was most unstable at all pH values except the highly acidic range (Figure 3a). Large agglomerates were observed at pH 5 which is near to the point of zero charge (pH_{zpc}), i.e. pH=5.6. Sodium citrate showed the greatest stabilization for almost all pH values except the highly acidic range (pH 1-3) because pH_{zpc} was shifted to these

values. No significant change was observed in the change of hydrodynamic size in pH 3-9 over the period of two weeks. The standard deviations of change in hydrodynamic diameter for three replicates show that there was inconsequential change, confirming the stability at a range of pH values. The control, PEG and PVP stabilized dispersion showed high aggregation rate at a pH value near to the point of zero charge (pH_{zpc}), as seen by the large aggregates near $pH_{zpc.}$

The point of zero charge for sodium citrate and SRFA was 1.6 and 2.3 respectively. The zeta potential for 0.3% SDS remained on negative values from pH1 up to pH10. The size change was fairly consistent with the positive and negative charge of the particles for all the surfactants over a period of two weeks. Generally the presence of negative charge on particles contributes to stabilising nanoparticles but this is not true with 0.3 mass percentage of SDS. This may be attributed to critical micelle concentration (CMC) of SDS which is 8.2 mM (0.00082%) in water at $25^{o}C$ and above which micelles form and all additional surfactants added to the system go to micelles [39].

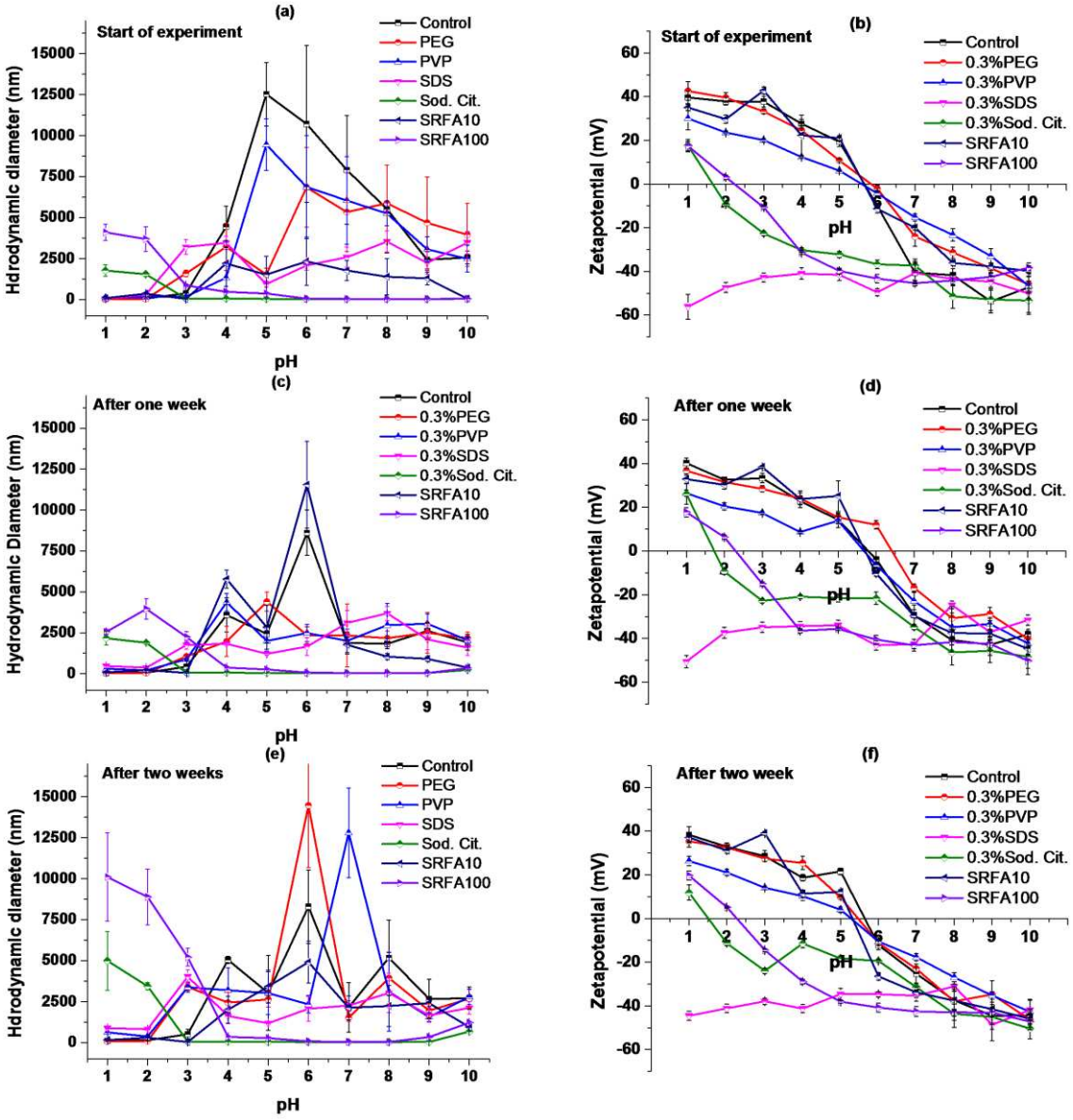

Figure 3: Effect of surfactants and pH on hydrodynamic diameter and zeta potential of 20ppm spherical anatase TiO_2 NP: a) Size at the start of experiment, b) Zeta potential at the start of experiment, c) Size after one week, d) Zeta potential after one week, e) Size after two weeks and f) Zeta potential after two weeks (All measurements were taken at pH 6.5±0.2 without any electrolyte).

A comparison of the zeta potential for 2 weeks (figure 3 b, d and f) showed no significant difference for all surfactants at all pH values except sodium citrate, which showed a slight increase in value at pH 4-7 (figure 3f). Consistency in zeta potential after 2 weeks shows that all sites on the particle surfaces are occupied by relevant charges which stabilized the hydrodynamic diameter and zeta

potential. This is also true for SRFA10 (i.e. 10 ppm SRFA) which was not able to provide enough negative charges to cover all particles and their surfaces. In comparison, SRFA100 (i.e. 100 ppm SRFA) provided enough concentration of charges to stabilize the dispersion. Sodium citrate (i.e. 0.3 weight percentage) and SRFA100 were used for below studies.

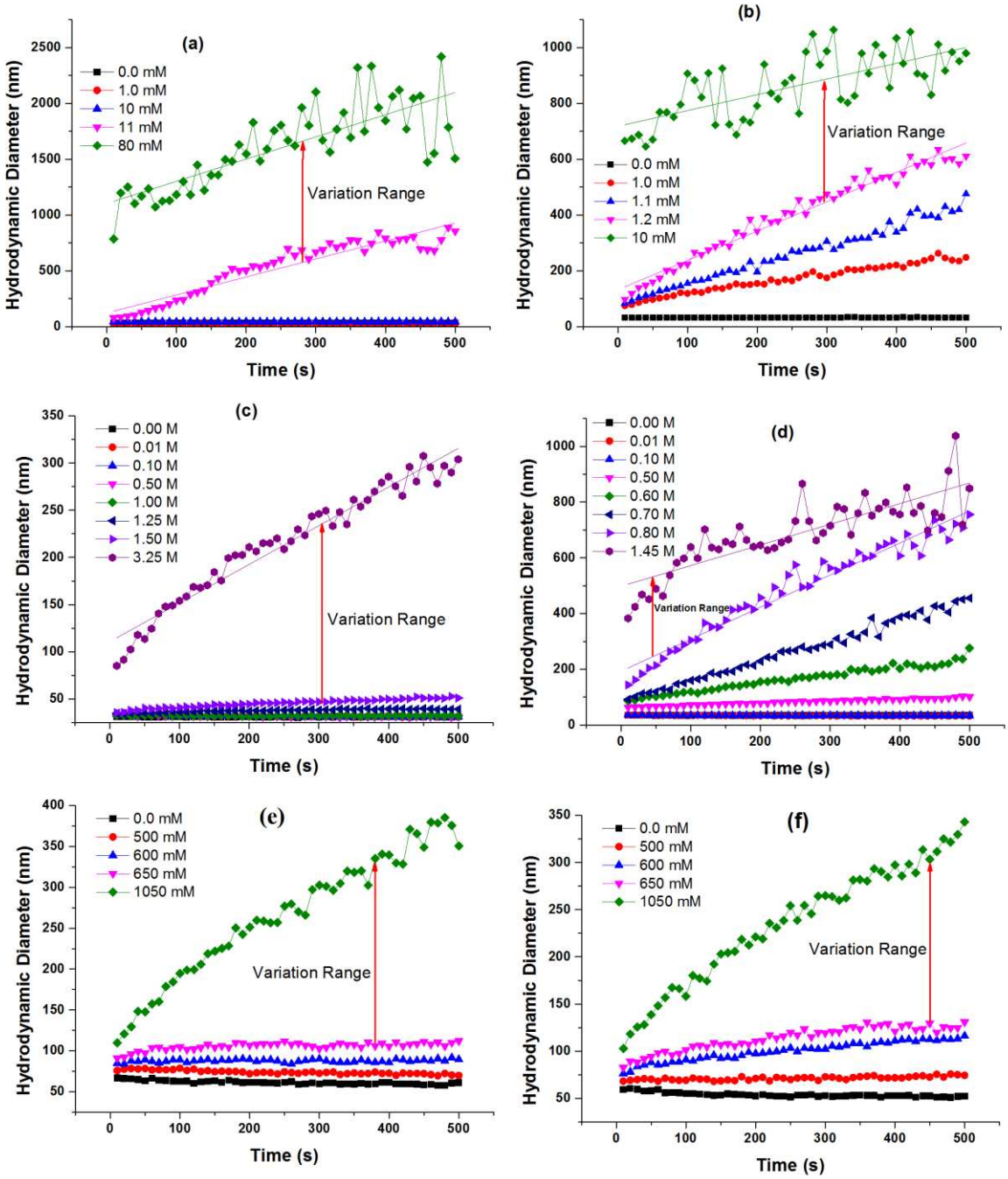

Figure 4: Effect of (a) $CaCl_2$ on sodium citrate stabilized ellipsoids; (b) $CaCl_2$ on SRFA stabilized ellipsoids; (c) NaCl on sodium citrate stabilized ellipsoids;(d) NaCl on SRFA stabilized ellipsoids; (e) NaCl on sodium citrate stabilized spherical NP and (f) NaCl on SRFA stabilized spherical NP (NP concentration of 20ppm, SRFA concentration of 100 ppm and pH=6.5±0.2)

Impact of ionic strength on the aggregation of TiO2 NP

The aggregation of nanoparticles showed a strong dependency on the ionic strength of the electrolyte dispersion. It was noted that with the addition of electrolytes, there was very slight change in pH values, i.e. ± 0.2, and the variation pH of the final dispersion was remained in the range of 6.5-7.0.

Impact on rutile ellipsoids

When treated with different salts, the rutile ellipsoids readily formed aggregates within 10 seconds of salt addition. During the first 10 seconds $Ca(NO_3)_2$ gave an average aggregate diameter of 585.4±22.9 nm and 530.3± 31.7 nm for sodium citrate and SRFA stabilized rutile ellipsoids respectively. Whereas the aggregates were slightly smaller in the case of $CaCl_2$ i.e. 531.9±5.1 nm and 366.1±4.9 nm for sodium citrate and SRFA stabilized ones respectively. For the sodium citrate stabilized ellipsoids treated with NaCl and $NaNO_3$ there was a very slight change in the initial hydrodynamic diameter with average diameter of 65.3±2.1nm and 59.8±0.2nm respectively. SRFA stabilized aggregates showed an average diameter of 247.7±20.2 nm and 190.8±2.9 nm for NaCl and $NaNO_3$respectively (Figure 4). Clearly the initial aggregate sizes in divalent salts (Figure 4 a and b) were larger than monovalent salts (Figure 4 c and d). Sodium citrate stabilized NP aggregation was entirely different than SRFA stabilized as CCC point reached quickly while in case of SRFA stabilized the CCC point reached slowly with addition of salts. Moreover the salt concentration variation range was much larger in case of sodium citrate stabilized NP as compared to SRFA stabilized (Figure 4). This is consistent with some previous reports showing quick formation of NP aggregates for different NP[21, 40, 41]. For example French et. al.[21] reported that 4−5 nm TiO_2 NP quickly formed stable aggregates of hydrodynamic diameter of 50−60 nm in presence of 0.0045 M NaCl at

pH of 4.5. At same pH value and 0.0165 M NaCl ionic strength, micron-sized aggregates were formed within 15 minutes. This time was decreased to 5 minutes at pH values 5.8−8.2 even at low NaCl ionic strength of 0.0084−0.0099 M. This aggregation time was 10 fold greater in an aqueous dispersion of 0.0128 M $CaCl_2$ and pH of 4.8. In another study Chen et. al.[36] studied that the divalent salts $CaCl_2$ and $MgCl_2$ gave much higher aggregate growth rate of alginate-coated hematite NP than that of monovalent NaCl. This process of aggregation was controlled by the thermodynamics where NP reduced their energies to form large aggregates. Figure 5 shows selected TEM micrographs of all salts used, which illustrates that there is an aggregate size and structural difference in the presence of monovalent (Figure 5 a&b) and divalent (Figure5 c&d) salts.

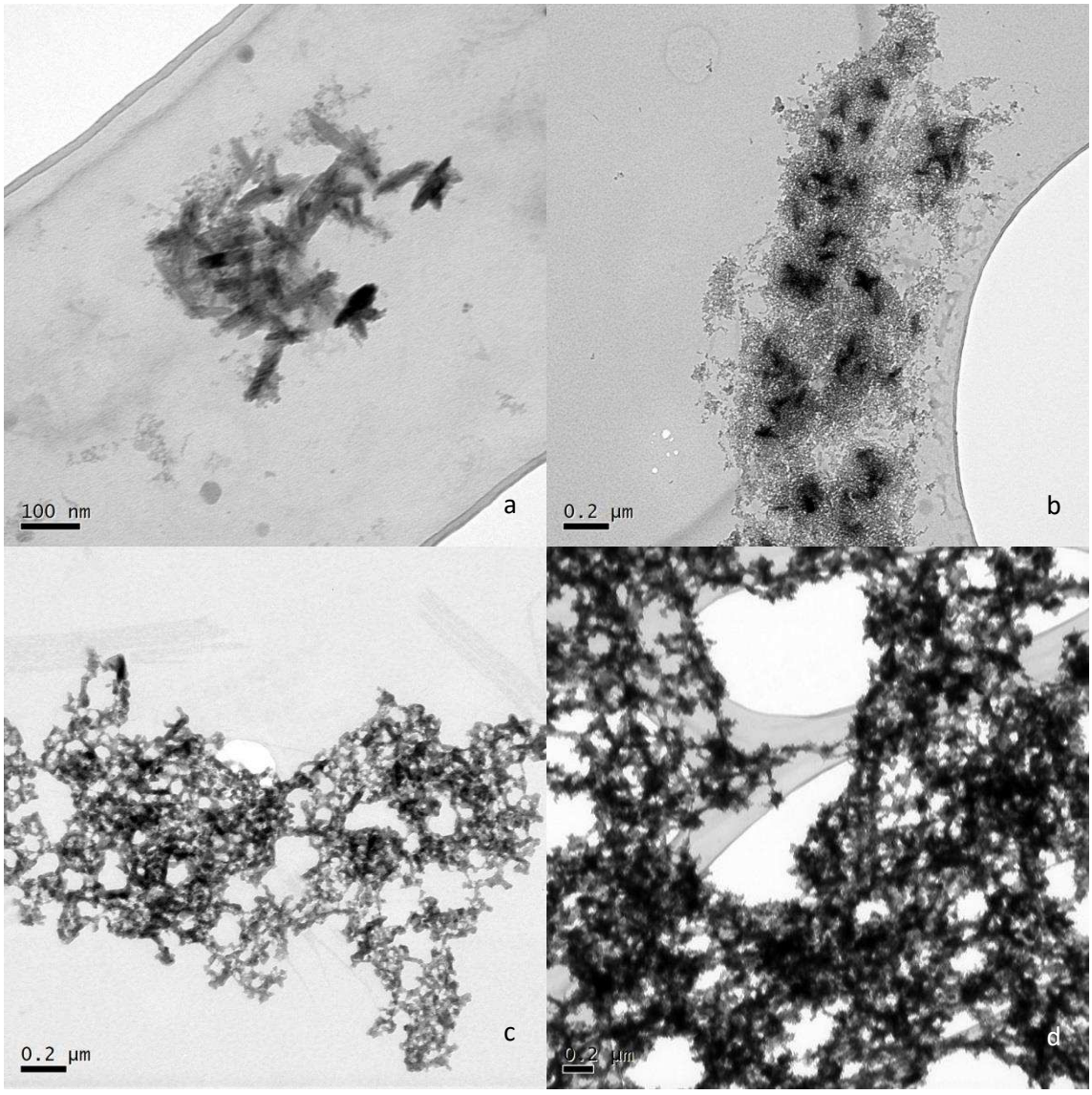

Figure 5: TEM images of aggregate formation behaviour and fractal dimensions of a) NaCl (1380mM) b) $NaNO_3$ (238mM) c) $Ca(NO_3)_2$ (16mM) d) $CaCl_2$ (10.7mM) on 20ppm sodium citrate stabilized TiO_2 ellipsoids (IS for these images corresponds to the CCC values represented in Table 1; pH=6.5±0.2).

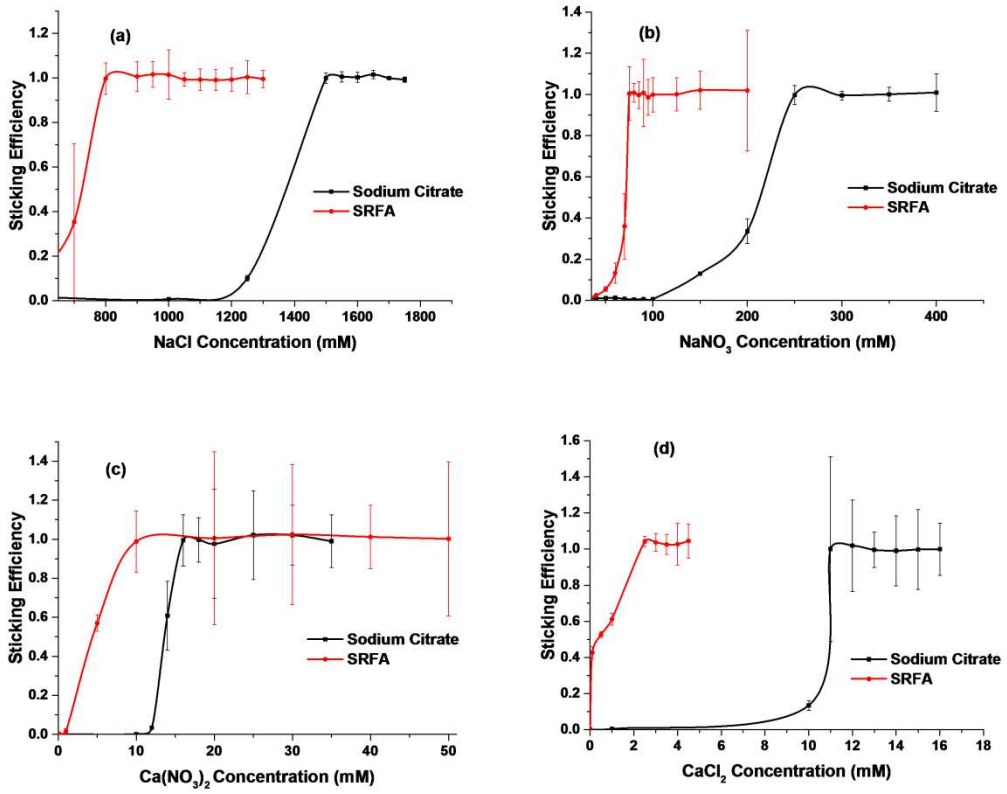

Figure 6: Sticking efficiency of sodium citrate and SRFA stabilized ellipsolids titania (20ppm) against a) NaCl b) $NaNO_3$ c) $Ca(NO_3)_2$ d) $CaCl_2$ (pH=6.5±0.2).

As shown in Figure 6, there is a general trend of destabilizing NP with the increase of salt concentration. For mono valence salts, the sodium citrate stabilized ellipsoids showed better stability with a critical coagulation concentration of 1380 ± 10 mM NaCl (Figure 6a). While for SRFA, the CCC was reduced to 790 mM NaCl (figure 6a). Similarly $NaNO_3$ gave the CCC of 238 mM for sodium citrate stabilized NP, which was much higher than SRFA stabilized NP with the CCC of 72 mM (Figure 6b).

The divalent ion behaved quite different from the monovalent salts. In the presence of $Ca(NO_3)_2$, the CCC was 16 mM (Figure 6c) for sodium citrate stabilized ellipsoids, which was reduced to 8.9 mM for SRFA stabilized NP. In the presence of $CaCl_2$, the CCC was observed as 10.7 mM and 4.2 mM for sodium citrate stabilized ellipsoids (figure 6d) and SRFA stabilized NP. While these results were similar in the general trend with the monovalent salts, the CCC values were much smaller, indicating that TiO_2 NP were more prone to be destabilized by the presence of divalent salts. The sticking efficiencies in the presence of monovalent salts showed a minimal rise as compared to divalent salts. It might be due to the degree of Debye-Hückel charge screening in monovalent salts is relatively less than divalent salts. This difference in CCCs is mainly because that Ca^{2+} ions have high efficiency to form complexes with citrate and fulvic acid[42]. It was noted that the CCCs of both SRFA and sodium citrate stabilized ellipsoids in the presence of divalent ions are much lower than the CCCs of monovalent salts. It is well documented that the dominant interacting mechanism is the interaction of Ca^{+2} ions with carboxyl groups in citrate, and the bridging complex with fulvic acid and humics characteristics are important from complex formation[36, 43-46]. Both of these reactions basically neutralized the stabilization effect hence causing quick destabilization of NP. Moreover this inequality of CCCs is most likely due to the lower tendency of monovalent cations to form complexes as compared to higher propensity of divalent cations, hence having higher CCC values.

When concentration of mono or divalent salt is increased gradually, the amount of charge screening increases, allowing an increase in aggregation kinetics. This type of aggregation is called reaction-limited aggregation. When the concentration of mono or divalent salts is very high, the charge of stabilized NP is fully screened eliminating the energy barrier between NP. Such an aggregation is called diffusion-limited aggregation where the aggregation kinetics approached to the maximum and is independent of the salt concentration. The CCC is actually the intersection of the cross-over point between both reaction and diffusion limited aggregation points. At high concentrations of mono and divalent salts, the overall charge of TiO_2 NP is totally screened and the energy barrier between NP is eliminated.

Impact on anatase spherical NP

The overall roundness of NP can be determined with a parameter called shape factor (α) which is defined as "the ratio of the surface area of a nonspherical nanoparticle (S^o) to that of a spherical nanoparticle (S), where both of the nanoparticle have identical volume, i.e. $\alpha = S^o/S$[47]. Due to many fluctuations in the aggregation behaviour of rutile ellipsoids as described above, round anatase NP with a shape factor of 0.9 or above were selected. The aggregation behaviour of round particles was different from the ellipsoids (Figure 5 and 7).

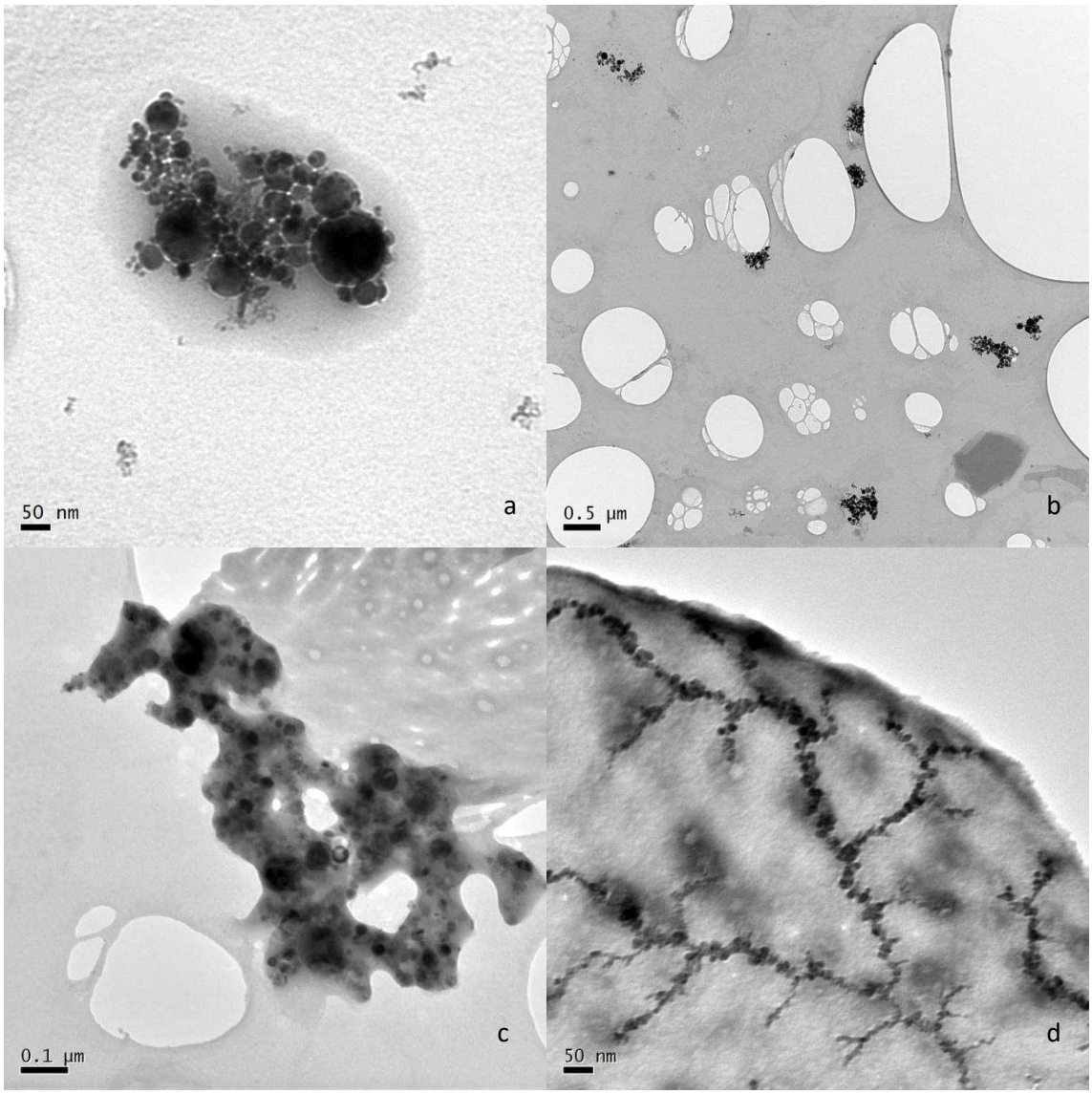

Figure 7: TEM images of aggregate formation behaviour and fractal dimensions of a) NaCl (900mM) b) $NaNO_3$ (90mM) c) $Ca(NO_3)_2$ (9.8mM) d) $CaCl_2$ (10.2mM) on 20ppm sodium citrate stabilized

spherical TiO_2 NP. (IS for these images corresponds to the CCC values represented in table 1; pH=6.5±0.2).

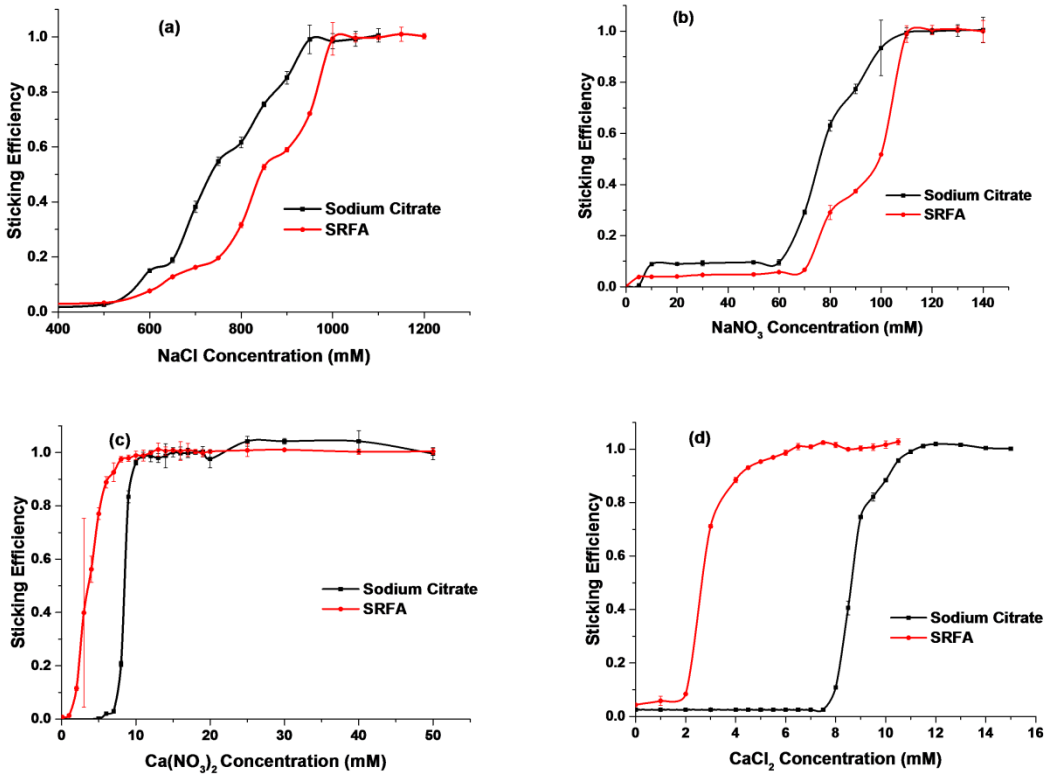

Figure 8: Sticking efficiency of sodium citrate and SRFA stabilized spherical anatase NP (20 ppm) against a) NaCl b) $NaNO_3$ c) $Ca(NO_3)_2$ d) $CaCl_2$ (pH=6.5±0.2)

For spherical TiO_2 NP, the results obtained from three measurements were more consistent, as shown by the small standard deviation values in Figure 8. In the presence of divalent salts, the agglomeration results were similar between spherical and ellipsoid TiO_2, where the CCC values were consistently lower for SRFA stabilized dispersions. However for monovalent salt, the CCC has shown smaller values for sodium citrate stabilized dispersions. For instance, the CCCs were 900 mM and 1025 mM respectively for sodium citrate and SRFA stabilized NP in the presence of NaCl. Similarly in the presence of $NaNO_3$, the CCC values were 90 mM and 115 mM respectively for sodium citrate and SRFA stabilized NP. A summary of the CCC values is provided in Table 1.

Table 1 Comparison of TiO_2 ellipsoids and spherical TiO_2 NP CCC values (20 ppm NP concentration)

Salt	Stabilizing agent	CCC (mM) ellipsoids	CCC (mM) spherical NP
NaCl	0.01% SRFA	790	1000
NaCl	0.3% Sod. citrate	1380	900
$NaNO_3$	0.01% SRFA	72	110
$NaNO_3$	0.3% Sod. citrate	238	90
$Ca(NO_3)_2$	0.01% SRFA	8.9	6.2
$Ca(NO_3)_2$	0.3% Sod. citrate	16	9.8
$CaCl_2$	0.01% SRFA	4.2	3.9
$CaCl_2$	0.3% Sod. citrate	10.7	10.2

DISCUSSIONS

Aggregation of TiO_2 nanomaterials in the presence of Sodium Chloride

The aggregation kinetics of TiO_2 NP in NaCl varied with the type of stabilizing agents. Results for sodium citrate stabilized titania ellipsoids reproduced in Fig 6a were in accordance with DLVO theory and gave a CCC of 1380 mM NaCl. This result was beyond the expectations but sodium citrate stabilized spheres also resulted in a CCC value of 790mM (Fig 6a & Table 1). However, the CCC for SRFA stabilized spherical NP was a bit higher than the CCC values ellipsoids (Fig 6a, 8a & Table 1).

There was an obvious difference in sticking efficiencies and the initial particle size of both types of SRFA stabilized nanomaterials. A change in NaCl concentration showed an obvious difference in the aggregates structure with a change of particle morphology (fig 6a, 8a & table 1). This observation is consistent with the observation made by Huynh et. al (2011) while treating spherical citrate-coated Ag NP with NaCl concentrations[44]. The current results show that sodium citrate stabilized ellipsoids have more stability against NaCl as compared to SRFA, while sodium citrate stabilized spherical NP showed lower CCC values compared to SRFA.

313 The stability and aggregation differences for two different shapes, i.e. spherical and ellipsoids are
314 mainly because of arrangement of stabilizing ions and polymer chains. These packing arrangements in
315 reaction and diffusion limited regimes for ellipsoids and spherical NP curvatures are shape specific
316 and give distinctiveness to each type[48].

317 In current research, the spherical TiO_2 NP have higher curvature as compared to the TiO_2 ellipsoids.
318 This detailed surface information alter the physical packing of the stabilizing agent resulting a more
319 compact layer of stabilizing agent for spherical NP as compared to more extended layer for the
320 ellipsoids. This arrangement of the stabilizing agent resulted in higher electrosteric interactions on the
321 curvatures of ellipsoids, giving them enhanced stability at reaction limited regime. While at diffusion
322 limited regime, the ellipsoids gave more stabilization because of higher physical packing with larger
323 amounts of cations.

324 Nanorods are proved to have higher physical packing hindrances as compared to small packing
325 density in nanospheres[49]. Thus electrosteric interactions at reaction limited regime and physical
326 hindrances arrangements of the stabilizing agent in diffusion limited regime are considered as
327 proposed mechanism for the morphological effect of nanoparticles on aggregation. So it is well
328 understood that this behaviour of ellipsoids is due to steric interactions for the particles having larger
329 aspect ratio. In one study on colloidal haematite, Boxall et al.[50] distinguished that dicarboxylic organic
330 acids provided steric effects and promoted aggregation.

331 It is well documented in the literature that the nanoparticles stabilized with carboxylic acids were
332 more homogenized and possess more negative surface charge as compared to those synthesized in
333 water alone[51]. So sodium citrate could influence more on the electrosteric effect in case of ellipsoids
334 with higher aspect ratios than spherical NP. In both cases of SRFA and sodium citrate, all NP
335 contained net negative charges which are being repelled by the negative counter ions on the
336 nanoparticles surface. This repulsion is more in case of ellipsoids due to increased surface area as
337 compared to counter ion effect of round NP.

Ellipsoids stabilized with SRFA exhibited aggregation behaviour quite similar to that for SRFA stabilized spherical NP (Figure 6a, 8a & Table 1). There was no obvious increase in the CCC both for ellipsoids and spherical NP stabilized with SRFA. SRFA may enhance particle stability by promoting electrosteric repulsion. The initial particle size of nanomaterial did not increase until the concentration of NaCl reached 500 mM for SRFA and 1250 mM for sodium citrate stabilized ellipsoids (Figure 4 c and d). In comparison, this growth started from 500 mM of NaCl for sodium citrate and SRFA stabilized spherical NP (Figure 4 e&f). These results clearly suggest the influence of aspect ratio, which enhanced stability of NP under same dispersion conditions. It is well documented that synthetic or natural stabilizing agents restrain electron transfer reactions because they reduce accessibility of the available surface area to stop reactions and increase stability[23, 52, 53].

Another reason for the stability of SRFA stabilized NP is the hydrophobicity of FA[54]. As per IHSS proton-binding study of the functional group charge densities, the phenol-carboxylic ratio of FA is 0.25 with a molecular weight of 500-2000 g/mol[54]. In this study NP stabilized with SRFA due to its greater hydrophobicity [55] and stronger steric repulsion [23]; resisted more to the addition of salts irrespective of the shape. TiO_2 ellipsoids with SRFA provided greater stability as compared to spherical NP under similar conditions.

Erhayem and Sohn[56] studied that adsorption of SRFA to the nano-TiO_2 surface was dependent on ionic strength regardless of the pH of media. With an increase in ionic strength, the SRFA would become more twisted and compact. This twisting might give some more nanoparticles surface area to be occupied by the SRFA giving a secondary stability. Therefore the amount of adsorption of SRFA on the surface of TiO_2 NP is highly dependent on the ionic strength. This twisting of the SRFA explains the higher stability of ellipsoids as compared to spherical NP because of more surface area of ellipsoids. At acidic pH, the TiO_2 surface has positive charges so cations give a bridging effect between positively-charged TiO_2 surface and negatively-charged SRFA, again imparting a secondary stability. Although this imparted stability loses its magnitude with increasing ionic strength, it might be a factor for the increased stability of ellipsoids due to increased surface area.

Aggregation of TiO_2 nanomaterials in the presence of Sodium Nitrate

The sodium citrate and SRFA stabilized titania nanomaterials behaved like NaCl aggregation when treated with $NaNO_3$. The CCC for citrate-coated nanoparticles in $NaNO_3$ was 72 mM (Figure 6b & Table 1) for SRFA stabilized ellipsoids which increased to 110mM for spherical NP (Figure 6b & Table 1). There was a drop in CCC, from a value of 238mM for titania ellipsoids (Figure 6b & Table 1) to 90mM $NaNO_3$ (Figure 8b & Table 1) which was similar to the value measured in case of NaCl. These CCC values are far less than NaCl CCC values although it was thought that both salts are mono-valent. As compared to NaCl, sodium citrate provided a degree of steric stability to the ellipsoids. The starting hydrodynamic size of the sodium citrate stabilized nanomaterials in $NaNO_3$, just like in NaCl, followed a decreasing trend with increasing electrolyte concentration initially (fig 6b & 8b). It was noted that the aggregate sizes were higher in high concentrations of $NaNO_3$ than in similar concentrations of NaCl, suggesting the effect of stabilizing agents was enhanced in $NaNO_3$ than in NaCl. Moreover, in the presence of NO_3^-, an open fractal structure was observed for the aggregated NP (Figure 7 b&d); however Cl^- gave closed fractal structures (Figure 7 a&c), which are the characteristics of aggregation under unfavorable circumstances. So NO_3^- always gave larger and open structures in all the cases and Cl^- gave smaller aggregate structures (Figure 5).

It was observed that CCC was different for differently stabilized NP and for NaCl or $NaNO_3$, which obviously suggests that the electrolyte anion have somehow very important role and it was not a ligand only. The role of anion was further confirmed by obvious differences in the aggregation of sodium citrate stabilized NP in NaCl and $NaNO_3$. The difference in the CCC and aggregation behaviour was not dependent on ion size, because the hydrated radius of Cl^- at 3.32 Å and NO^{-3} at 3.35 Å[57] are quite close and might not be able to give much difference in behaviour. It might be NO^{-3} which made the gel like complexes with SRFA and sodium citrate. CCC values of two types of anions reveal that anion effect depends on the type of electrolyte. Stability of TiO_2 ellipsoids and spherical NP is affected at very low concentrations of Cl^- and NO^{3-} for divalent salts while huge amount of Cl^- was required to destabilize both types of NP in case of NaCl. As Ca^+ always form a gel-like aggregates [36] and NO_3 forms open fractal branched structures, $Ca(NO_3)_2$ make larger aggregates as

compared to monovalent salts or divalent Ca^{+} with Cl^{-}. This is well confirmed while observing the sticking efficiencies where monovalent electrolytes gave more stability with higher CCC values. The combined effect of the gel-like aggregates effect of Ca^{+} with the open fractal structures of NO_3^{-} is the possible reason of larger aggregate size and lower CCC values for $Ca(NO_3)_2$. The aggregation state in all cases is related to the overall surface area, adsorption of anion and the sorbate surface exposure. CCC results showed that the greater the attraction of anions by TiO_2 surface, the lower is the stability and vice versa.

Aggregation of TiO_2 nanomaterials in the presence of Calcium Nitrate

$Ca(NO_3)_2$ showed aggregation behaviour which was quite in line with $NaNO_3$ (Table 1). No changes were observed between CCC values of both types of NP but these CCC values are far less than $NaNO_3$ CCC value, which was attributed to Ca^{+2} because of its quick screen of surface charge by divalent ions. This enhancement in aggregation might be due to the compression of the electrical diffused double layer on TiO_2 NP surface as a result of chelation between NP surface and Ca^{2+}. The results show that the CCC for the SRFA stabilized TiO_2 NP (either ellipsoids or spherical) was at least an order of magnitude higher than sodium citrate coated NP.

Both type of TiO_2 NP either coated with SRFA or sodium citrate had negative zeta potential values. With the addition of divalent calcium cations, the zeta potential of stabilized NP decreased. It is well documented in literature that Ca^{2+} forms a complex with organic matter stabilized hematite NP, which neutralized the negative surface charge of the NP[36]. In the presence of divalent Ca^{2+}, same mechanism governs the destabilization of both types of NP. SRFA imparted the negative charge on the surface of both types of TiO_2 NP. These imparted negative charges made complex with Ca^{2+} to destabilize the NP dispersion even with little amounts of the divalent salt.

Aggregation of TiO_2 nanomaterials in the presence of Calcium Chloride

The aggregation behaviour observed in $CaCl_2$ was similar to that observed in NaCl but the NP started to aggregate at a lower concentration of $CaCl_2$. The stability of the SRFA stabilized nanomaterials in $CaCl_2$ was obviously different from that in NaCl, as divalent cations quickly changed

417 the aggregation stage. The ellipsoids either stabilized by sodium citrate or SRFA showed a better
418 magnitude of stability as compared to spherical NP mainly due to the greater surface area. This clearly
419 illustrates the effect of shape on the stability of NP. The high charge screening efficiency of Ca^{+2} ions
420 for the nanomaterials could be the possible aggregation mechanisms along with the specific
421 interaction of nanomaterials, Ca^{+2} ions and stabilizing agents[58].

422 Huynh and Chen[44] considered the interparticle bridging of NP by interaction of humic acid and Ca^{2+}
423 ions as the main reason of aggregation. They emphasized that polymer coated NP had more stability
424 as compared to citrate coated NP in the presence of monovalent and divalent ions. This is more likely
425 because of the electrosteric stability induced by large chain polymers. The sticking of SRFA
426 molecules imparted additional stability to the NP in the presence of low concentrations of ions. But
427 when the concentration was high, the intermolecular bridging induced by SRFA gave enhanced
428 aggregation.

429 CONCLUSIONS

430 This study showed that the surfactant, ionic strength and morphology of TiO_2 NP affected the
431 aggregation kinetics significantly. Five surfactants were investigated influencing the aggregation
432 process but sodium citrate and SRFA were the most effective stabilizing agents. NP morphology has
433 influenced the sticking efficiency and crystal structure, which altered the aggregation kinetics TiO_2
434 ellipsoids proved more resistant to aggregation than spherical NP against different Ca^{+2} and Na^{+} salts
435 at similar concentrations. Salt concentrations changed the sticking efficiency between individual NP
436 and NP-substrate surfaces. It is considered that the aggregation kinetics is due to Ca^{+2} and Na^{+} cations
437 but CO_3^{-} and Cl^{-} anions may also have their impacts, which will be studied in future work.

438 ENVIRONMENTAL IMPLICATIONS

439 SRFA stabilized NP are relatively more stable than sodium citrate stabilized NP, mainly due to the
440 electrosteric repulsion by the SRFA molecules. Since the CCC values for both types of NP are greater
441 than typical environmental related concentrations of mono and divalent salt concentrations, it is

presumed that these NP are highly mobile in natural environments. Moreover natural environments have fulvic and humic acids in abundance which naturally increase the stability of these NP hence increasing their mobility. This work acts as a benchmark study to understand the ultimate fate of engineered nanoparticles in the environment. Clearly due to the complexities in real soil matrix, which would have different complex nature of ions and natural organic matters, understanding the real time fate of engineered nanoparticles is still a big challenge. Clearly there is still a strong need of further studies to establish the influence of other environmental constituents like natural organic matters, humic acids and different metals on the aggregation kinetics of titania NP. In addition, further research work is needed to assess the effect of different sizes and phase contents on NP stability, aggregation kinetics and mobility.

AUTHOR INFORMATION

***Corresponding Authors**

Phone: +44 113 343 1299, Email: d.wen@leeds.ac.uk

Phone: +44 113 343 2350, Email: g.raza@leeds.ac.uk

Acknowledgement

This work was supported by European Research Council Consolidator Grant (Grant number: 648375).

References

(1. Rao, C. N. R.; Müller, A.; Cheetham, A. K., *The chemistry of nanomaterials*. Wiley. com: 2006; Vol. 1.

2. Gottschalk, F.; Sonderer, T.; Scholz, R. W.; Nowack, B., Modeled environmental concentrations of engineered nanomaterials (TiO2, ZnO, Ag, CNT, fullerenes) for different regions. *Environmental Science & Technology* **2009**, *43*, (24), 9216-9222.

3. Tsuji, J. S.; Maynard, A. D.; Howard, P. C.; James, J. T.; Lam, C.-w.; Warheit, D. B.; Santamaria, A. B., Research Strategies for Safety Evaluation of Nanomaterials, Part IV: Risk Assessment of Nanoparticles. *Toxicological Sciences* **2006**, *89*, (1), 42-50.

4. Grass, R. N.; Tsantilis, S.; Pratsinis, S. E., Design of high-temperature, gas-phase synthesis of hard or soft TiO2 agglomerates. *AIChE Journal* **2006**, *52*, (4), 1318-1325.

5. Mandzy, N.; Grulke, E.; Druffel, T., Breakage of TiO2 agglomerates in electrostatically stabilized aqueous dispersions. *Powder Technology* **2005**, *160*, (2), 121-126.

6. Kretzschmar, R.; Schäfer, T., Metal Retention and Transport on Colloidal Particles in the Environment. *Elements* **2005**, *1*, (4), 205-210.

7. Kataoka, S.; Gurau, M. C.; Albertorio, F.; Holden, M. A.; Lim, S.-M.; Yang, R. D.; Cremer, P. S., Investigation of Water Structure at the TiO2/Aqueous Interface. *Langmuir* **2004**, *20*, (5), 1662-1666.

8. Klaine, S. J.; Alvarez, P. J. J.; Batley, G. E.; Fernandes, T. F.; Handy, R. D.; Lyon, D. Y.; Mahendra, S.; McLaughlin, M. J.; Lead, J. R., Nanomaterials in the environment: Behavior, fate, bioavailability, and effects. *Environmental Toxicology and Chemistry* **2008**, *27*, (9), 1825-1851.

9. Chen, J.; Xiu, Z.; Lowry, G. V.; Alvarez, P. J. J., Effect of natural organic matter on toxicity and reactivity of nano-scale zero-valent iron. *Water Research* **2011**, *45*, (5), 1995-2001.

10. Edgington, A. J.; Roberts, A. P.; Taylor, L. M.; Alloy, M. M.; Reppert, J.; Rao, A. M.; Mao, J.; Klaine, S. J., The influence of natural organic matter on the toxicity of multiwalled carbon nanotubes. *Environmental Toxicology and Chemistry* **2010**, *29*, (11), 2511-2518.

11. Wang, C.-y.; Bahnemann, D. W.; Dohrmann, J. K., A novel preparation of iron-doped TiO2 nanoparticles with enhanced photocatalytic activity. *Chemical Communications* **2000**, (16), 1539-1540.

12. Mylon, S. E.; Chen, K. L.; Elimelech, M., Influence of Natural Organic Matter and Ionic Composition on the Kinetics and Structure of Hematite Colloid Aggregation: Implications to Iron Depletion in Estuaries. *Langmuir* **2004**, *20*, (21), 9000-9006.

13. Dunnivant, F. M.; Schwarzenbach, R. P.; Macalady, D. L., Reduction of substituted nitrobenzenes in aqueous solutions containing natural organic matter. *Environmental Science & Technology* **1992**, *26*, (11), 2133-2141.

14. Navarro, E.; Baun, A.; Behra, R.; Hartmann, N.; Filser, J.; Miao, A.-J.; Quigg, A.; Santschi, P.; Sigg, L., Environmental behavior and ecotoxicity of engineered nanoparticles to algae, plants, and fungi. *Ecotoxicology* **2008**, *17*, (5), 372-386.

15. Zhang, W., Nanoparticle aggregation: principles and modeling. In *Nanomaterial*, Springer: 2014; pp 19-43.

16. Allen, L. H.; Matijević, E., Stability of colloidal silica: I. Effect of simple electrolytes. *Journal of Colloid and Interface Science* **1969**, *31*, (3), 287-296.

17. Pfeiffer, C.; Rehbock, C.; Hühn, D.; Carrillo-Carrion, C.; de Aberasturi, D. J.; Merk, V.; Barcikowski, S.; Parak, W. J., Interaction of colloidal nanoparticles with their local environment: the (ionic) nanoenvironment around nanoparticles is different from bulk and determines the physico-chemical properties of the nanoparticles. *Journal of the Royal Society Interface* **2014**, *11*, (96), 20130931.

18. Wang, J.; Mishra, A. K.; Zhao, Q.; Huang, L., Size effect on thermal stability of nanocrystalline anatase TiO2. *Journal of Physics D: Applied Physics* **2013**, *46*, (25), 255303.

19. Zhang, H.; Gilbert, B.; Huang, F.; Banfield, J. F., Water-driven structure transformation in nanoparticles at room temperature. *Nature* **2003**, *424*, (6952), 1025-1029.

20. Dunphy Guzman, K. A.; Finnegan, M. P.; Banfield, J. F., Influence of Surface Potential on Aggregation and Transport of Titania Nanoparticles. *Environmental Science & Technology* **2006**, *40*, (24), 7688-7693.

21. French, R. A.; Jacobson, A. R.; Kim, B.; Isley, S. L.; Penn, R. L.; Baveye, P. C., Influence of Ionic Strength, pH, and Cation Valence on Aggregation Kinetics of Titanium Dioxide Nanoparticles. *Environmental Science & Technology* **2009**, *43*, (5), 1354-1359.

22. Logtenberg, E. H. P.; Stein, H. N., Surface charge and coagulation of aqueous ZnO dispersions. *Journal of Colloid and Interface Science* **1986**, *109*, (1), 190-200.

23. Domingos, R. F.; Tufenkji, N.; Wilkinson, K. J., Aggregation of Titanium Dioxide Nanoparticles: Role of a Fulvic Acid. *Environmental Science & Technology* **2009**, *43*, (5), 1282-1286.

24. Sun, J.; Guo, L.-H.; Zhang, H.; Zhao, L., UV Irradiation Induced Transformation of TiO2 Nanoparticles in Water: Aggregation and Photoreactivity. *Environmental Science & Technology* **2014**, *48*, (20), 11962-11968.

25. Jassby, D.; Farner Budarz, J.; Wiesner, M., Impact of Aggregate Size and Structure on the Photocatalytic Properties of TiO2 and ZnO Nanoparticles. *Environmental Science & Technology* **2012**, *46*, (13), 6934-6941.

26. Gumy, D.; Morais, C.; Bowen, P.; Pulgarin, C.; Giraldo, S.; Hajdu, R.; Kiwi, J., Catalytic activity of commercial of TiO2 powders for the abatement of the bacteria (E. coli) under solar simulated light: Influence of the isoelectric point. *Applied Catalysis B: Environmental* **2006**, *63*, (1–2), 76-84.

27. Chowdhury, I.; Cwiertny, D. M.; Walker, S. L., Combined Factors Influencing the Aggregation and Deposition of nano-TiO2 in the Presence of Humic Acid and Bacteria. *Environmental Science & Technology* **2012**, *46*, (13), 6968-6976.

28. Amirkhani, M.; Volden, S.; Zhu, K.; Glomm, W. R.; Nyström, B., Adsorption of cellulose derivatives on flat gold surfaces and on spherical gold particles. *Journal of Colloid and Interface Science* **2008**, *328*, (1), 20-28.

29. Keller, A. A.; Wang, H.; Zhou, D.; Lenihan, H. S.; Cherr, G.; Cardinale, B. J.; Miller, R.; Ji, Z., Stability and Aggregation of Metal Oxide Nanoparticles in Natural Aqueous Matrices. *Environmental Science & Technology* **2010**, *44*, (6), 1962-1967.

30. Thio, B. J. R.; Zhou, D.; Keller, A. A., Influence of natural organic matter on the aggregation and deposition of titanium dioxide nanoparticles. *Journal of Hazardous Materials* **2011**, *189*, (1–2), 556-563.

31. Mwaanga, P.; Carraway, E.; Schlautman, M., Preferential sorption of some natural organic matter fractions to titanium dioxide nanoparticles: influence of pH and ionic strength. *Environ Monit Assess* **2014**, *186*, (12), 8833-8844.

32. Klitzke, S.; Metreveli, G.; Peters, A.; Schaumann, G. E.; Lang, F., The fate of silver nanoparticles in soil solution — Sorption of solutes and aggregation. *Science of The Total Environment*, (0).

33. Zhou, H.; Zou, Z.; Wu, S.; Ge, F.; Li, Y.; Shi, W., Rapid synthesis of TiO2 hollow nanostructures with crystallized walls by using CuO as template and microwave heating. *Materials Letters* **2011**, *65*, (6), 1034-1036.

34. Zhou, D.; Keller, A. A., Role of morphology in the aggregation kinetics of ZnO nanoparticles. *Water Research* **2010**, *44*, (9), 2948-2956.

35. Yin, H.; Wada, Y.; Kitamura, T.; Sumida, T.; Hasegawa, Y.; Yanagida, S., Novel synthesis of phase-pure nano-particulate anatase and rutile TiO2 using TiCl4 aqueous solutions. *Journal of Materials Chemistry* **2002**, *12*, (2), 378-383.

36. Chen, K. L.; Mylon, S. E.; Elimelech, M., Aggregation Kinetics of Alginate-Coated Hematite Nanoparticles in Monovalent and Divalent

Electrolytes. *Environmental Science & Technology* **2006**, *40*, (5), 1516-1523.

37. Kim, A. Y.; Berg, J. C., Fractal Aggregation: Scaling of Fractal Dimension with Stability Ratio. *Langmuir* **1999**, *16*, (5), 2101-2104.

38. Garzella, C.; Comini, E.; Tempesti, E.; Frigeri, C.; Sberveglieri, G., TiO2 thin films by a novel sol–gel processing for gas sensor applications. *Sensors and Actuators B: Chemical* **2000**, *68*, (1–3), 189-196.

39. IUPAC, Compendium of Chemical Terminology Gold Book. **2014**, *Dated 2014-02-24*, (Version 2.3.3).

40. Wang, P.; Keller, A. A., Natural and Engineered Nano and Colloidal Transport: Role of Zeta Potential in Prediction of Particle Deposition. *Langmuir* **2009**, *25*, (12), 6856-6862.

41. Sousa, V. S.; Teixeira, M. R., Aggregation kinetics and surface charge of CuO nanoparticles: the influence of pH, ionic strength and humic acids. *Environmental Chemistry* **2013**, *10*, (4), 313-322.

42. Baalousha, M.; Nur, Y.; Römer, I.; Tejamaya, M.; Lead, J. R., Effect of monovalent and divalent cations, anions and fulvic acid on aggregation of citrate-coated silver nanoparticles. *Science of The Total Environment* **2013**, *454–455*, (0), 119-131.

43. Gutierrez, L.; Aubry, C.; Cornejo, M.; Croue, J.-P., Citrate-Coated Silver Nanoparticles Interactions with Effluent Organic Matter: Influence of Capping Agent and Solution Conditions. *Langmuir* **2015**, *31*, (32), 8865-8872.

44. Huynh, K. A.; Chen, K. L., Aggregation Kinetics of Citrate and Polyvinylpyrrolidone Coated Silver Nanoparticles in Monovalent and Divalent Electrolyte Solutions. *Environmental science & technology* **2011**, *45*, (13), 5564-5571.

45. Kalinichev, A. G.; Iskrenova-Tchoukova, E.; Ahn, W.-Y.; Clark, M. M.; Kirkpatrick, R. J., Effects of Ca2+ on supramolecular aggregation of natural organic matter in aqueous solutions: A comparison of molecular modeling approaches. *Geoderma* **2011**, *169*, 27-32.

46. Kirishima, A.; Tanaka, K.; Niibori, Y.; Tochiyama, O., Complex formation of calcium with humic acid and polyacrylic acid. *Radiochim. Acta* **2002**, *90*, (9-11), 555-561.

47. Qi, W. H.; Wang, M. P.; Liu, Q. H., Shape factor of nonspherical nanoparticles. *Journal of Materials Science* **2005**, *40*, (9-10), 2737-2739.

48. Fazio, G.; Ferrighi, L.; Di Valentin, C., Spherical versus Faceted Anatase TiO2 Nanoparticles: A Model Study of Structural and Electronic Properties. *The Journal of Physical Chemistry C* **2015**, *119*, (35), 20735-20746.

49. Rudge, J.; Holness, M.; Smith, G., Quantitative textural analysis of packings of elongate crystals. *Contrib Mineral Petrol* **2008**, *156*, (4), 413-429.

50. Boxall, A. B.; Tiede, K.; Chaudhry, Q., Engineered nanomaterials in soils and water: how do they behave and could they pose a risk to human health? *Nanomedicine* **2007**, *2*, (6), 919-927.

51. Chang, X.; Vikesland, P. J., Effects of carboxylic acids on nC60 aggregate formation. *Environmental Pollution* **2009**, *157*, (4), 1072-1080.

52. EU, Commission recommendation of 18 October 2011 on the definition of nanomaterial *Official Journal L* **2011**, *275*, 38-40.

53. Li, S.; Sun, W., A comparative study on aggregation/sedimentation of TiO2 nanoparticles in mono- and binary systems of fulvic acids and Fe(III). *Journal of Hazardous Materials* **2011**, *197*, (0), 70-79.

54. Baalousha, M.; Motelica-Heino, M.; Coustumer, P. L., Conformation and size of humic substances: Effects of major cation concentration and type, pH, salinity, and residence time. *Colloids and Surfaces A: Physicochemical and Engineering Aspects* **2006**, *272*, (1–2), 48-55.

55. Westerhoff, P.; Mezyk, S. P.; Cooper, W. J.; Minakata, D., Electron Pulse Radiolysis Determination of Hydroxyl Radical Rate Constants with Suwannee River Fulvic Acid and Other Dissolved Organic Matter Isolates. *Environmental Science & Technology* **2007**, *41*, (13), 4640-4646.

56. Erhayem, M.; Sohn, M., Stability studies for titanium dioxide nanoparticles upon adsorption of Suwannee River humic and fulvic acids and natural organic matter. *Science of The Total Environment* **2014**, *468–469*, 249-257.

57. Richards, L. A.; Richards, B. S.; Schäfer, A. I., Renewable energy powered membrane technology: Salt and inorganic contaminant removal by nanofiltration/reverse osmosis. *Journal of Membrane Science* **2011**, *369*, (1–2), 188-195.

58. Konradi, R.; Rühe, J., Interaction of Poly(methacrylic acid) Brushes with Metal Ions: Swelling Properties. *Macromolecules* **2005**, *38*, (10), 4345-4354.